Materials Science & Engineering A 601 (2014) 153–158

Contents lists available at ScienceDirect

Materials Science & Engineering A

journal homepage: www.elsevier.com/locate/msea

Enhancing dislocation emission in nanocrystalline materials through shear-coupled migration of grain boundaries

Jianjun Li [a,*], A.K. Soh [b], Xiaolei Wu [c]

[a] Department of Engineering Mechanics, School of Mechanics, Civil Engineering and Architecture, Northwestern Polytechnical University, Xi'an, Shanxi, People's Republic of China
[b] School of Engineering, Monash University Sunway Campus, Malaysia
[c] LNM, Institute of Mechanics, Chinese Academy of Sciences, No. 15, Beisihuanxi Road, Beijing 100190, People's Republic of China

ARTICLE INFO

Article history:
Received 22 October 2013
Received in revised form
13 February 2014
Accepted 15 February 2014
Available online 20 February 2014

Keywords:
Nanocrystalline materials
Dislocations
Shear-coupled migration of grain boundaries
Strength and ductility

ABSTRACT

A theoretical model has been developed to illustrate the effect of shear-coupled migration of grain boundaries on dislocation emission in nanocrystalline materials. The energy characteristics and critical shear stress τ_c that is required to initiate the emission process were determined. The results obtained show that the dislocation emission can be considerably enhanced as shear-coupled migration was the dominating process; a critical coupling factor that corresponded to the minimum τ_c, which led to an optimal dislocation emission, was also discovered. The proposed model has also been quantitatively validated by the existing molecular dynamics simulations.

1. Introduction

Intensive investigations in the past decades have shown that the remarkable physical and mechanical properties of nanocrystalline (NC) materials such as ultrahigh strength and hardness are usually gained at the expense of their ductility, which is limited to a few percent of uniform elongation [1,2]. The brittle behavior of NC materials is attributed to the suppression of conventional dislocation slips, which are dominating in their coarse-grained counterparts, as the grain size is reduced to nanoscale [1–7]. Meanwhile, various NC specimens that possessed both high strength and ductility have been reported [8–19]; moreover, it has been proposed that the outstanding balance was due to some grain boundaries (GBs)-mediated deformation mechanisms, such as GB sliding, emission of dislocations from GBs and GB migration [16–20]. Furthermore, enormous dislocation activities were discovered in the grain interiors of some NC samples in experiments [10,21–23] and the accumulation of such dislocations in the grain interior due to the formation of Lomer–Cottrell locks [22] led to their exceptional strain hardening and ductility. However, what remains unclear is the mechanism that leads to the emission of abundant dislocations, which form Lomer–Cottrell locks and, hence, developing a good synergy of high strength and ductility in these NC materials.

Among all the GB-mediated deformation modes, stress-driven shear-coupled migration of grain boundaries is an important and generic mode of plastic deformation and athermal grain growth in NC materials, as demonstrated by many molecular dynamics simulations, quasi-continuum studies as well as experiments and theories [24–30]. It is interesting to note that the grain size of the NC sample investigated in Ref. [22] was increased from 25 nm to 38 nm while the strain was increased from 0 to 1, which suggests that shear-coupled migration of grain boundaries might have played an important role in enhancing dislocation emission and hence achieving the strong strain hardening characteristic in the sample. This athermal process [20] normally consists of a normal GB migration accompanied by a tangential translation of grains parallel to the GB plane for both low-angle and high-angle boundaries; the process would then produce shear deformation of the lattice traversed by the migrated GB. The translation distance s is related to the normal migration distance m by a coupling factor $\beta = s/m$ [31]. The value of β is determined by the geometry of the GB concerned [31,32], and the maximum value of β can reach 1 based on experiments [27,33] and MD simulations [25,32] and reach 5 according to theoretical studies [34,35]. The coupled mode has been revealed as a very effective toughening mechanism in NC materials [36] and it can considerably enhance the intrinsic ductility of NC materials by incorporating with the conventional GB sliding process [37].

Moreover, Sansoz and Dupont [26] conducted an indentation study for an NC Al thin film of 7 nm grain size at 0 K using the quasicontinuum method. Their results showed that some partials

* Corresponding author. Tel.: +86 13259738949; fax: +86 2988431000.
E-mail addresses: jianjunli.mech@gmail.com, mejjli@nwpu.edu.cn (J. Li).

http://dx.doi.org/10.1016/j.msea.2014.02.044
0921-5093

could emit from disclinated GBs and stacking faults were formed after dislocation emission during the process of shear-coupled grain boundary motion (refer to Fig. 2f–g in Ref. [26]). This observation has also been made by a recent MD study of Schafer and Albe [25] on a uniaxial tensile deformation of an NC copper sample of 10 nm average grain size at room temperature (refer to Fig. 3 in Ref. [25]). Some experiments carried out by De Hosson et al. [38,39] and Mompiou et al. [27,40] have also shown that dislocations activity was promoted during the motion of grain boundary in bicrystal or ultrafine-grained metals and that the moving GBs acted as a source of dislocations. Most recently, Ovid'ko and Skiba [41] proposed theoretically that dislocations could emit approximately vertically from a disclinated GB fragment generated by GB sliding or migration. However, the coupled shear in the migration process was ignored and only one slip system was incorporated in their study. Therefore, the main aim of this paper is to identify the role of the coupled shear (via the coupling factor β) in enhancing the dislocation emission in NC materials and to describe the shear-coupled migration as a new mode of emitting dislocations in NC materials. In order to provide a more realistic simulation of NC materials, it is assumed that multiple slip systems are activated and both the leading and trailing partials are movable in the proposed model according to the observations made in experiments and MD studies [25,26,45] on the emission process of dislocations from GBs.

2. Geometry of dislocation emission induced by shear-coupled migration of grain boundaries

Consider a deformed elastically isotropic NC specimen in two dimensions consisting of a large amount of nanograins and GBs subjected to a remote tensile stress σ, as shown in Fig. 1a. For simplicity, only a typical two-grain structure is considered (Fig. 1b). The applied stresses are assumed to be sufficiently high to initiate a shear-coupled migration of the GB 'AB' between two grains G1 and G2, which are in light and dark gray colors, respectively, as shown in Fig. 1b. Assume that the GB 'AB' is migrated to a rectangular grain ABDC (i.e., G2 in Fig. 1b) in the form of migration normal to GB 'AB' by a distance m, which is simultaneously accompanied by a tangential translation $s=\beta m$ ($\beta=$ tan φ) that is parallel to the GB 'AB' plane (Figs. 1c and 2). Therefore, the initial GB 'AB' is moved to a new location, i.e., $A'B'$. In accordance with the theory of defects in solids, the shear-coupled migration process would lead to the formation of two dipoles of wedge disclination, i.e., $AA'$and BB' of arm l and strength $\pm\omega$. This shear-coupled migration of GB 'AB' simultaneously gives rise to an increase and a decrease of size of grains G1 and G2, respectively (Fig. 1c). For simplicity, the length of GB 'AB' (i.e., d) can be taken as the approximate grain size of the NC specimen.

The high stresses induced by the two disclination dipoles coupled with the action of the external stress could enable the emission of multiple dislocations from the two disclinated GB fragments AA' and BB' into grain G1 after growth (as shown in the light gray grain in Fig. 1c). For simplicity, we assume that the emission process generates two dipoles of Shockley dislocations of the edge, 90°-type in a face-centered cubic lattice. One dipole of partials with Burgers vectors $\mathbf{b_1}$ and $-\mathbf{b_1}$ is emitted from the disclinated GB AA', which are called $\pm b_1$ dipole dislocations, whereas the partials of the other dipole with Burgers vectors $\mathbf{b_2}$ and $-\mathbf{b_2}$ are emitted from the disclinated GB fragment BB', which are called the $\pm b_2$ dipole dislocations (Fig. 1c). The magnitude of Burgers vector of the two dipole partials is assumed to be the same in the present analysis, i.e., $b_1=b_2=a/\sqrt{6}$, where a is the lattice parameter. All the partial dislocations are assumed to be able to glide in the grain G1 of increased size. The $\pm b_1$-dipole slips along

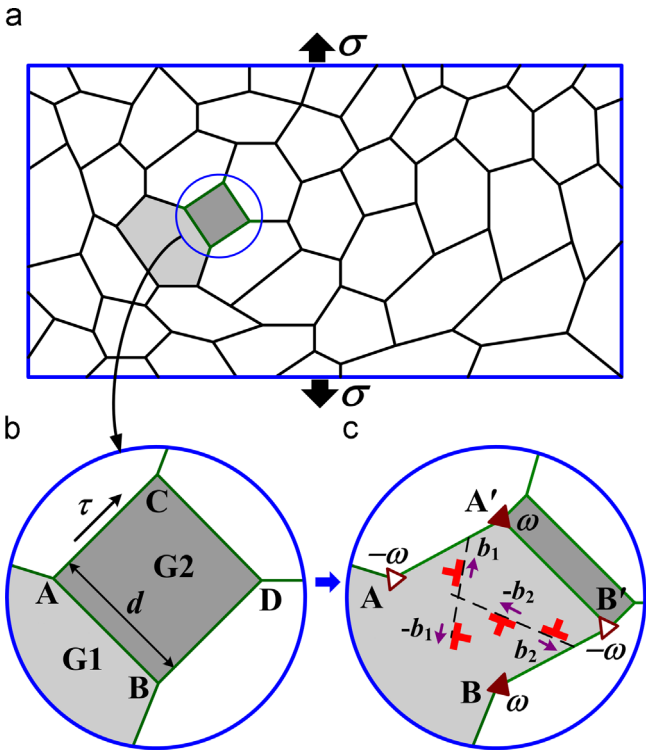

Fig. 1. Lattice dislocation emission in a nanocrystalline specimen in which shear-coupled migration of grain boundaries (GBs) is dominating: (a) general view; (b) initial configuration of GBs; and (c) configuration resulting from the shear-coupled migration of GB 'AB' accompanied by the emission of two partial dislocation dipoles, i.e., $\pm b_1$ and $\pm b_2$ dipoles from the disclinated GB fragments AA' and BB', respectively, into grain G1 of increased size.

a crystallographic plane that inclines at an angle θ_1 (called emission angle 1) with the disclinated GB AA', while the $\pm b_2$-dipole slides along another plane that inclines at an angle θ_2 (called emission angle 2) with the disclinated GB BB'. Two stacking faults of lengths p and q are formed after the emission and motion of the two dipoles, as schematically shown by the zigzags in Fig. 2; p_1 and q_1 are the glide distance of the two trailing partials in the two dipoles; h_1 and h_2 are defined as the distances between the two dislocation emission sources and the two positive disclinations, i.e., A′ and B, in the disclinated GBs AA' and BB', respectively, as shown in Fig. 2, for the sake of convenience in deriving the expression of the energy changes in the following section; and α is the angle between the two dipoles.

3. Energy characteristics of dislocation emission due to shear-coupled migration process

Let us examine the change in energy ΔW resulting from the dislocation emission process, which is the difference in energy between the initial state of the system containing two disclination dipoles generated by the shear-coupled migration of GB 'AB' before the dislocation emission and that after the emission. The process of dislocation emission is energetically favorable if $\Delta W<0$. The energy change ΔW (per unit length along the axis perpendicular to the plane of Fig. 1c) can be expressed as follows:

$$\Delta W = E^b + E^\gamma + E_{\text{int}}^{\omega-b} + E_{\text{int}}^{b_1-b_2} - A \tag{1}$$

where E^b is the dipole energy of the $\pm b_1$ and $\pm b_2$ dipole dislocations; E^γ is the energy of the two stacking fault strips; $E_{\text{int}}^{\omega-b}=E_{\text{int }1}^{\omega-b_1}+E_{\text{int }2}^{\omega-b_1}+E_{\text{int }1}^{\omega-b_2}+E_{\text{int }2}^{\omega-b_2}$ is the energy that characterizes the interaction between the dislocation dipoles and the disclination

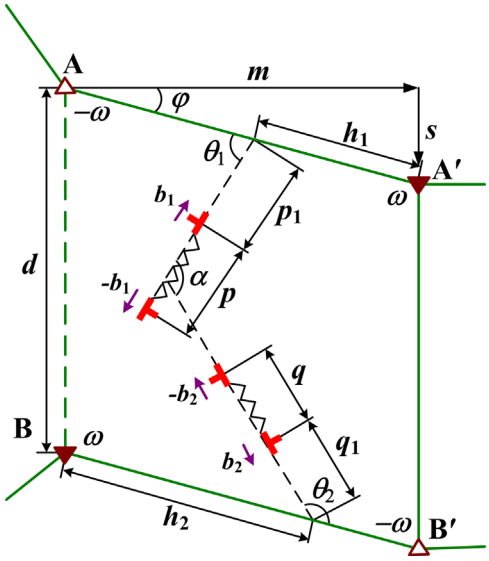

Fig. 2. Geometrical parameters during the process of dislocation emission after shear-coupled grain boundary migration, as shown in Fig. 1 (c).

dipoles, where $E_{\text{int }1}^{\omega-b_1}$ and $E_{\text{int }2}^{\omega-b_1}$ are the energy terms resulting from the interaction between the $\pm b_1$ dislocation dipole and the disclination dipoles AA' and BB', respectively; $E_{\text{int }1}^{\omega-b_2}$ and $E_{\text{int }2}^{\omega-b_2}$ are those resulting from the interaction between the $\pm b_2$ dislocation dipole and the disclination dipoles AA' and BB', respectively, and A is work done by the external shear stress τ to glide the two dipoles.

Let us calculate the above terms for an NC specimen with shear modulus G and Poisson's ratio ν. The dipole energy of $\pm b_1$ and $\pm b_2$ dislocations is given as [42]

$$E^b = Db_1^2\left(\ln\frac{p-r_{c1}}{r_{c1}}+1\right)+Db_2^2\left(\ln\frac{q-r_{c2}}{r_{c2}}+1\right) \tag{2}$$

where $D=G/2\pi(1-\nu)$ and $r_{c1}\approx b_1$ and $r_{c2}\approx b_2$ are the dislocation core radii for $\pm b_1$ and $\pm b_2$ dislocations, respectively. The stacking fault energy can be expressed as $E^{\gamma}=\gamma_{\text{st}}(p+q)$, where γ_{st} is the specific energy of the stacking fault per unit area, where p and q are the lengths of the $\pm b_1$ and $\pm b_2$ dipoles, respectively. The work done by the external shear stress τ to glide the two dipoles is $A=\tau pb_1\cos(2\theta_1-2\varphi)-\tau qb_2\cos(2\theta_2-2\varphi)$, for which the direction of the shear stress τ is parallel to the GB 'AC' and pointing to the triple junction C (Fig. 1b). The energy $E_{\text{int }1}^{\omega-b_1}$ is calculated in a standard manner [42,43] as the work done in generating the $\pm b_1$ dislocation dipole in the stress field created by the disclination dipole AA', which can be expressed as follows after some mathematical treatment:

$$E_{\text{int }1}^{\omega-b_1}=\frac{D\omega b_1\sin\theta_1}{2}\Big[h_1\ln(x^2+2xh_1\cos\theta_1+h_1^2)-(h_1-l)\ln(x^2+2x(h_1-l)\cos\theta_1+(h_1-l)^2)\Big]_{x=(p_1+p)}^{x=p_1} \tag{3}$$

Similarly, $E_{\text{int }2}^{\omega-b_1}$, $E_{\text{int }1}^{\omega-b_2}$ and $E_{\text{int }2}^{\omega-b_2}$ can be formulated as follows:

$$E_{\text{int }2}^{\omega-b_1}=\frac{D\omega b_1\sin\theta_1}{2}\Big[h_1'\ln(x^2+2xh_1'\cos\theta_1+h_1'^2)-(h_1'-l)\ln(x^2+2x(h_1'-l)\cos\theta_1+(h_1'-l)^2)\Big]_{x=(p_2+p)}^{x=p_2} \tag{4}$$

$$E_{\text{int }1}^{\omega-b_2}=\frac{D\omega b_2\sin\theta_2}{2}\Big[h_2'\ln(x^2+2xh_2'\cos\theta_2+h_2'^2)-(h_2'-l)\ln(x^2+2x(h_2'-l)\cos\theta_2+(h_2'-l)^2)\Big]_{x=(q_2+q)}^{x=q_2} \tag{5}$$

$$E_{\text{int }2}^{\omega-b_2}=\frac{D\omega b_2\sin\theta_2}{2}\Big[h_2\ln(x^2+2xh_2\cos\theta_2+h_2^2)-(h_2-l)\ln(x^2+2x(h_2-l)\cos\theta_2+(h_2-l)^2)\Big]_{x=(q_1+q)}^{x=q_1} \tag{6}$$

where $l=m/\cos\varphi$, $p_2=d\cos\varphi/\sin\theta_1-p_1-p$, $h_1'=l-h_1-d\cos(\varphi-\theta_1)/\sin\theta_1$, $\theta_2=\pi+\theta_1-\alpha$, $q_2=d\cos\varphi/\sin\theta_2-q_1-q$, $h_2'=l-h_2-d\cos(\varphi-\theta_2)/\sin\theta_2$, and h_1, h_2, p_1, q_1 are shown in Fig. 2. The energy $E_{\text{int}}^{b_1-b_2}$ can be calculated as the work done in generating the $\pm b_2$ dipole in the stress field created by the $\pm b_1$ dipole and it is described by

$$\begin{aligned}E_{\text{int}}^{b_1b_2}=&Db_1b_2\Big[\frac{\cos\alpha}{2}\ln A_1-\frac{f_1I_1}{2\sin^2\alpha}(2+\cos 2\alpha)\cos^2\alpha\\&-\frac{f_1}{2A_1\sin^2\alpha}[x(2+\cos\alpha\cos 3\alpha)+f_1(2+\cos 2\alpha)\cos\alpha]\Big]_{x=(e_1+q)}^{x=e_1}\\&-Db_1b_2\Big[\frac{\cos\alpha}{2}\ln A_2-\frac{f_2I_2}{2\sin^2\alpha}(2+\cos 2\alpha)\cos^2\alpha\\&-\frac{f_2}{2A_2\sin^2\alpha}[x(2+\cos\alpha\cos 3\alpha)\\&+f_2(2+\cos 2\alpha)\cos\alpha]\Big]_{x=(e_1+q)}^{x=e_1}\end{aligned} \tag{7}$$

where $b_1=b_2=a/\sqrt{6}$, $f_1=-(e+0.5p)$, $f_2=-(e-0.5p)$, $e=(h_2'-h_1)\sin\theta_2/\sin\alpha+p/2-p_1$, $e_1=(h_2-h_1')\sin\theta_1/\sin\alpha-q_1-q$ $A_1=x^2+2xf_1\cos\alpha+f_1^2$, $A_2=x^2+2xf_2\cos\alpha+f_2^2$, $I_1=\arctan[(x+f_1\cos\alpha)/(f_1\sin\alpha)]/(f_1\sin\alpha)$ and $I_2=\arctan[(x+f_2\cos\alpha)/f_2\sin\alpha]/(f_2\sin\alpha)$.

By combining Eqs. (1)–(7), the total energy change ΔW can be determined as follows:

$$\begin{aligned}\Delta W=&\frac{D\omega b_1\sin\theta_1}{2}\Big[h_1\ln(x^2+2xh_1\cos\theta_1+h_1^2)-(h_1-l)\ln(x^2+2x(h_1-l)\cos\theta_1+(h_1-l)^2)\Big]_{x=(p_1+p)}^{x=p_1}\\&+\frac{D\omega b_1\sin\theta_1}{2}\Big[h_1'\ln(x^2+2xh_1'\cos\theta_1+h_1'^2)-(h_1'-l)\ln(x^2+2x(h_1'-l)\cos\theta_1+(h_1-l)^2)\Big]_{x=(p_2+p)}^{x=p_2}\\&+\frac{D\omega b_2\sin\theta_2}{2}\Big[h_2\ln(x^2+2xh_2\cos\theta_2+h_2^2)-(h_2-l)\ln(x^2+2x(h_2-l)\cos\theta_2+(h_2-l)^2)\Big]_{x=(q_1+q)}^{x=q_1}\\&+\frac{D\omega b_2\sin\theta_2}{2}\Big[h_2'\ln(x^2+2xh_2'\cos\theta_2+h_2'^2)-(h_2'-l)\ln(x^2+2x(h_2'-l)\cos\theta_2+(h_2'-l)^2)\Big]_{x=(q_2+q)}^{x=q_2}\\&+Db_1b_2\Big[\frac{\cos\alpha}{2}\ln A_1-\frac{f_1I_1}{2\sin^2\alpha}(2+\cos 2\alpha)\cos^2\alpha\\&-\frac{f_1}{2A_1\sin^2\alpha}[x(2+\cos\alpha\cos 3\alpha)+f_1(2+\cos 2\alpha)\cos\alpha]\Big]_{x=(e_1+q)}^{x=e_1}\\&-Db_1b_2\Big[\frac{\cos\alpha}{2}\ln A_2-\frac{f_2I_2}{2\sin^2\alpha}(2+\cos 2\alpha)\cos^2\alpha\\&-\frac{f_2}{2A_2\sin^2\alpha}[x(2+\cos\alpha\cos 3\alpha)+f_2(2+\cos 2\alpha)\cos\alpha]\Big]_{x=(e_1+q)}^{x=e_1}\\&+Db_1^2\left(\ln\frac{p-r_{c1}}{r_{c1}}+1\right)+Db_2^2\left(\ln\frac{q-r_{c2}}{r_{c2}}+1\right)+\gamma_{\text{st}}(p+q)\\&-\tau[pb_1\cos(2\theta_1-2\varphi)-qb_2\cos(2\theta_2-2\varphi)]4\end{aligned} \tag{8}$$

An NC Al sample of $G=26.5$ GPa [44], $\nu=0.345$ [44], $\gamma_{st}=122\ mJ\ m^{-2}$ [45] and $a\approx 0.404$ nm [45] is selected for the following calculations. Other parameters are set as $d=30$ nm, $m=1$ nm, and $\tau=0.8$ GPa.

4. Results and discussion

Firstly, the energy change $\Delta W(p,\theta_1)$ (in units of eV/nm) of an NC Al sample of 30 nm grain size for different coupling factors, i.e., $\beta=0$, 0.5 and 1.5, are plotted in Fig. 3a–c, respectively. The values

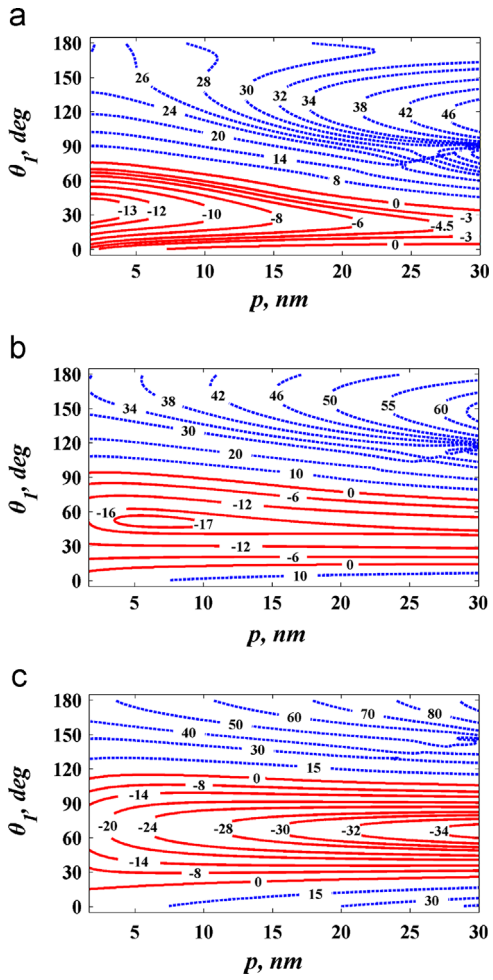

Fig. 3. Contours of energy change $\Delta W(p,\theta_1)$ (in units of eV/nm) characterizing the process of dislocation emission from two disclinated GB fragments in a nanocrystalline Al of 30 nm grain size at $\tau=0.8$ GPa, $\omega=0.8$, $\alpha=2\pi/3$, $m=1$ nm, $q=10$ nm, $p_1=q_1=0$ and $h_1=h_2=l/2$ for various values of coupling factors, i.e., (a) $\beta=0$ (pure migration); (b) $\beta=0.5$; and (c) $\beta=1.5$.

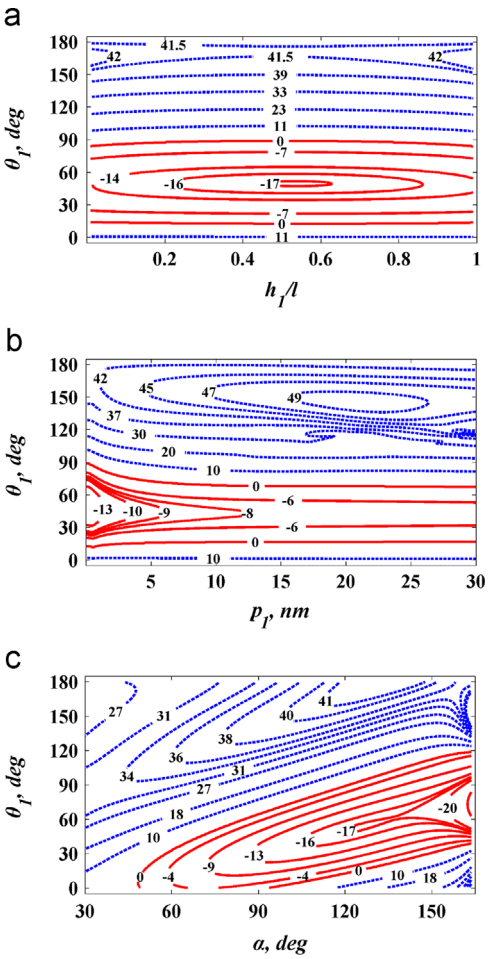

Fig. 4. Contours of energy change $\Delta W(h_1/l,\theta_1)$ (a), $\Delta W(p_1,\theta_1)$ (b) and $\Delta W(\alpha,\theta_1)$ (c) (in units of eV/nm) for a 30 nm nanocrystalline Al at $\tau=0.8$ GPa, $\omega=0.8$, $\beta=0.5$, $m=1$ nm, $p=q=10$ nm, $q_1=0$ and $h_2=l/2$. Other parameters are taken as $p_1=0$, $\alpha=2\pi/3$ in (a), $h_1=l/2$, $\alpha=2\pi/3$ in (b) and $p_1=0$, $h_1=l/2$ in (c).

of the parameter h_1 and h_2 are set as one half of l (i.e., $h_1=h_2=l/2$); and p_1 and q_1 are set as zero, which is assumed based on our latter results, which showed that the mentioned value would be able to ensure that the energy change could reach a minimum for all values of other parameters, see Fig. 4a and b. Other parameters are set as $\tau=0.8$ GPa, $\omega=0.8$, $\alpha=2\pi/3$, $m=1$ nm, $q=10$ nm. It can be seen from Fig. 3 that the zone of p and θ_1 at which $\Delta W(p,\theta_1)$ is negative enlarges drastically with increasing β, as indicated by the solid lines in Fig. 3, from which we obtain that: (i) the minimum value of ΔW is reduced considerably, i.e., from -13 to -34 with the increase of β from 0 to 1.5 (Fig 3a and c); (ii) the magnitude of p increases from 0 nm to 30 nm, i.e., the grain size and the value of θ_1 corresponding to the minimum ΔW increases from 35° to around 67° with the increase of β from 0 to 1.5 (Fig. 3a and c), which suggests that the leading $(-b_1)$-dislocation has moved across the whole grain G1 and could arrive not only at the opposite GB BB' but also at all other GBs of G1, thus considerably enhancing the possibility of its interaction with the $\pm b_2$ dislocation and hence the formation of Lomer–Cottrell locks; and (iii) the range of θ at $p=30$ nm increases from 30° to 80° (i.e., a factor of larger than 2.6) when β is raised from 0 to 1.5 (Fig. 3a and c). The above results indicate that the dislocation emission process is energetically more favorable, as shear-coupled migration is the dominating process compared with pure normal migration and that the coupled shear (i.e., $\beta>0$) is able to considerably enhance the dislocation emission in NC materials, which is in good agreement with the existing observations made in experiments [27,38–40], MD and quasicontinuum studies [25,26].

In order to consider the effect of some geometrical parameters on the energy change, the contours of $\Delta W(h_1/l,\theta_1)$, $\Delta W(p_1,\theta_1)$ and $\Delta W(\alpha,\theta_1)$ (in units of eV/nm) for nanocrystalline Al of 30 nm grain size at $\tau=0.8$ GPa, $\omega=0.8$, $\beta=0.5$, $m=1$ nm, $p=q=10$ nm, $q_1=0$ and $h_2=l/2$ are plotted in Fig. 4a–c, respectively. The results obtained show that the energy change reaches its minimum as $h_1=l/2$, $p_1=0$, and that the larger the value of α, the smaller the energy change is. The contours of $\Delta W(h_2/l,\theta_1)$ and $\Delta W(p_2,\theta_1)$ are not shown in the figure due to their similarity to those of $\Delta W(h_1/l,\theta_1)$ and $\Delta W(p_1,\theta_1)$. Therefore, in the following calculation, the values of h_1, h_2 are set as $l/2$ and p_1, q_1 are set to 0.

Fig. 5 presents the variation of minimum energy change $\Delta W_{\min}$ (in units of eV/nm) with respect to the disclination strength ω for a 30 nm nanocrystalline Al sample at $\tau=0.8$ GPa for various values of β based on the results presented in Fig. 3. Other parameters are taken as $h_1=h_2=l/2$, $p_1=q_1=0$, $q=10$ nm, $\alpha=2\pi/3$. It can be seen that the value of $\Delta W_{\min}$ for the dislocation emission process induced by the shear-coupled migration process (i.e., the case of $\beta=0.5$, 1 and 1.5) is much smaller than that for the case of pure migrations (i.e., $\beta=0$) and the reduction of $\Delta W_{\min}$ increases with increasing β.

It is also of vital importance to calculate the critical stress τ_c that is defined as the minimum external shear stress at which the process of dislocation emission from the two disclinated GB

fragments AA' and BB' is energetically favorable. This can be done by considering the critical condition $\Delta W(\tau_c, \beta, \alpha, \theta_1,\ p_1 = p_{1\,\min}, q_1 = q_{1\,\min}, p = p_{\min}, q = q_{\min}) = 0$, where $p_{1\,\min}$ and $q_{1\,\min}$ are the least glide distance of the two trailing partials in the two dipoles and their values could be zero, i.e., $p_{1\,\min} = q_{1\,\min} = 0$; $p_{\min}$ and $q_{\min}$ are the minimum length of the two stacking faults and their values could be several times of the dislocations core radius, such as $p_{\min} = q_{\min} \approx 10 r_{c1}$, as assumed in the present study. Since the energy change usually reaches a minimum at $h_1 = h_2 = l/2$, as shown in Fig. 4a, the values of h_1 and h_2 are set as half of the value of the disclination dipole length l. As a result, τ_c is a function of θ_1, β and α, and it varies with θ_1. Minimization of τ_c with respect to θ_1 is performed to determine $\tau_c(\beta, \alpha)$. Fig. 6 presents the variation of τ_c versus the coupling factor β in the interval of $[0, 2]$ for different disclination strengths, i.e., $\omega = 0.1$, 0.3 and 0.5, for an NC Al sample of 30 nm grain size. It is obvious that the value of τ_c for the dislocation emission process induced by the shear-coupled migration in the NC specimen (i.e., $\beta > 0$) is much smaller than that for the case of pure migration (i.e., $\beta = 0$). Another interesting finding is that there exists a critical β, i.e., β_c, which corresponds to the minimum τ_c for each ω, as indicated by the small circles in the curves. The values of β_c for various ω are approximately the same, e.g., $\beta_c = 0.96$ for $\omega = 0.1$, 0.3 and $\beta_c = 0.91$ for $\omega = 0.5$. These values of β_c are easily accessible from both experimental studies and molecular dynamics simulations for nanocrystalline solids [25,27,32]. The effect of β can be quantitatively specified by the ratio $\tau_c(\beta = 0)/\tau_c(\beta = \beta_c)$, which increases from 1.06 to 2.17 as ω increases from 0.1 to 0.5. This result indicates that the coupled shear (i.e., the coupling factor β) plays an important role in enhancing the dislocation activity in nanocrystalline materials, which consist of mostly high-angle boundaries (i.e., $\omega > 0.26$) [1]. This finding provides a possible explanation for the abundant dislocation activity observed in the experiments conducted by De Hosson et al. [38,39] and Mompiou et al. [27,40] for nano-grained and ultrafine-grained Al during nano-indentation or tensioning where grain boundary motions played a significant role. Since the value of β depends on the specific structure of GBs, the results obtained from Fig. 6 suggest that it is possible to stimulate an optimal dislocation emission in NC materials through engineering the GB structure in order to obtain the β_c.

To validate the proposed model, the critical shear stress τ_c for a nanocrystalline copper sample of 10 nm grain size is calculated, as shown in Fig. 7, which shows the variation of τ_c with respect to α. The material parameters are taken as $G = 39.6$ GPa [6], $\upsilon = 0.36$, $\gamma_{st} = 55\ mJ\ m^{-2}$ [46], a $\approx 0.362\ nm$ [47]. The values of the coupling factor and migration distance are adopted from the work of Schafer and Albe [25], i.e., $\beta = 0.5$, $m = 2$ nm. The results obtained show that τ_c first decreases, then increases, and finally decreases with increasing α. In the MD simulations performed by Schafer and Albe [25] on uniaxial tensile deformation of an NC Cu sample with 10 nm grain size, they found that the dislocation activities were highly enhanced and many of them were emitted from disclinated GBs. The stress–strain curves as well as the evolution of dislocation density with strain are presented in their Fig. 2 for a pure NC Cu sample. In the present model, four partial dislocations are assumed to be emitted into the grain interior with increased size of 12 nm, which leads to a dislocation density of $0.33 \times 10^{16}/\mathrm{m}^2$. This value of dislocation density corresponds to a strain of 7.38% and in return a flow stress of 1.88 GPa (refer to Fig. 2 in Ref. [25]). Considering the relation between the tensile and shear stresses, the corresponding critical shear stress obtained from the MD simulations performed by Schafer and Albe [25] should be half of the flow stress, i.e., 0.94 GPa. This value is also presented in Fig. 7 for comparison, which shows that the model prediction at $\alpha \approx 101^{\circ}$ is in good agreement with the MD results at -as shown by the circle in Fig. 7.

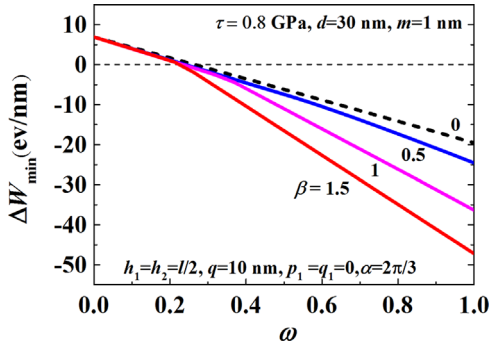

Fig. 5. Variation of the minimum energy change $\Delta W_{\min}$ with the disclination strength ω for a 30 nm nanocrystalline Al at $\tau = 0.8$ GPa for various coupling factors β.

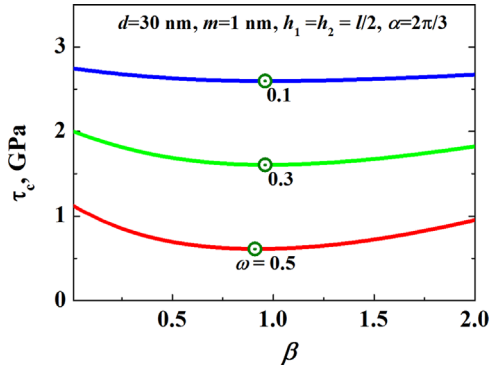

Fig. 6. Variation of the critical stress τ_c with coupling factor β for a 30 nm nanocrystalline Al at $m = 1$ nm, $h_1 = h_2 = l/2$ and $\alpha = 2\pi/3$ with various values of disclination strength considered. The circles on the lines represent the critical coupling factor β_c corresponding to the minimum τ_c.

5. Conclusions

In summary, dislocation emission in NC materials can be highly enhanced through shear-coupled migration of grain boundaries. The range of the emission angle 1 (θ_1) and the length (p) of the stacking fault, at which the energy change is negative, increase with increasing value of the coupling factor β. Moreover, the coupling shear is able to drastically decrease the minimum value of energy change. The critical shear stress τ_c for initiating the dislocation emission process can be reduced significantly due to

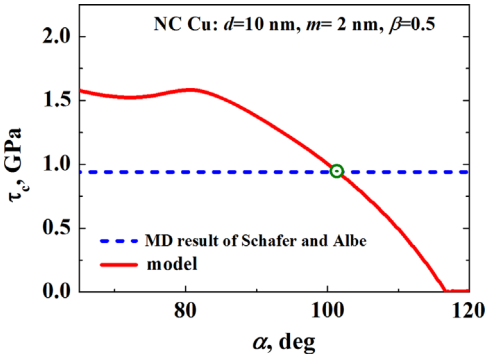

Fig. 7. Comparison of the critical stress τ_c with respect to α between model predictions and MD results obtained by Schafer and Albe [25] for a 10 nm nanocrystalline Cu specimen. The values of the migration distance and coupling factor are adopted from the work of Schafer and Albe [25], i.e., $m = 2$ nm and $\beta = 0.5$.

the existence of coupled shear during the migration process, especially in the case of high-angle boundary; and it is important to note that there is a critical coupling factor β_c that corresponds to the minimum τ_c, which indicates that the dislocations in NC materials can possibly be maximized by engineering the GB structure to obtain an appropriate value of β [31,33]. The predicted critical shear stress for initiating multiple dislocations that emit from disclinated GBs into grain interiors in multiple slip systems has also been validated by the existing MD simulations for a nanocrystalline Cu sample of 10 nm grain size. Thus, we propose to tune the GB structure to generate the largest amount of dislocations for achieving an optimal strength/ductility balance in NC materials.

Acknowledgments

J. Li acknowledges the financial support of Start-up funding for the Newly-recruited High-level Talents of Northwestern Polytechnical University, People's Republic of China. A.K. Soh acknowledges the support of eScience funding (Project no.: 06-02-10-SF0195) from MOSTI (Malaysia) and the Advanced Engineering Programme and School of Engineering, Monash University Sunway Campus.

References

[1] M.A. Meyers, A. Mishra, D.J. Benson, Prog. Mater. Sci. 51 (2006) 427–556.
[2] M. Dao, L. Lu, R.J. Asaro, J.T.M. De Hosson, E. Ma, Acta Mater. 55 (2007) 4041–4066.
[3] H. Gleiter, Prog. Mater. Sci. 33 (1989) 223–315.
[4] Y. Champion, S. Guerin-Mailly, J.L. Bonnentien, P. Langlois, Scr. Mater. 44 (2001) 1609–1613.
[5] Y.M. Wang, K. Wang, D. Pan, K. Lu, K.J. Hemker, E. Ma, Scr. Mater. 48 (2003) 1581–1586.
[6] P.G. Sanders, J.A. Eastman, J.R. Weertman, Acta Mater. 45 (1997) 4019–4025.
[7] K.S. Siow, A.A.O. Tay, P. Oruganti, Mater. Sci. Technol. 20 (2004) 285–294.
[8] Y. Wang, E. Ma, R.Z. Valiev, Y. Zhu, Adv Mater 16 (2004) 328–331.
[9] Y. Wang, E. Ma, M. Chen, Appl. Phys. Lett. 80 (2002) 2395.
[10] K.M. Youssef, R.O. Scattergood, K.L. Murty, J.A. Horton, C.C. Koch, Appl. Phys. Lett. 87 (2005) 091904.
[11] K.M. Youssef, R.O. Scattergood, K.L. Murty, C.C. Koch, Scr. Mater. 54 (2006) 251–256.
[12] Y.H. Zhao, T. Topping, J.F. Bingert, J.J. Thornton, A.M. Dangelewicz, Y. Li, W. Liu, Y.T. Zhu, Y.Z. Zhou, E.L. Lavernia, Adv. Mater. 20 (2008) 3028–3033.
[13] Y.H. Zhao, J.E. Bingert, X.Z. Liao, B.Z. Cui, K. Han, A.V. Sergueeva, A.K. Mukherjee, R.Z. Valiev, T.G. Langdon, Y.T.T. Zhu, Adv. Mater. 18 (2006) 2949.
[14] S. Cheng, E. Ma, Y.M. Wang, L.J. Kecskes, K.M. Youssef, C.C. Koch, U.P. Trociewitz, K. Han, Acta Mater. 53 (2005) 1521–1533.
[15] Y. Champion, C. Langlois, S. Guerin-Mailly, P. Langlois, J.L. Bonnentien, M.J. Hytch, Science 300 (2003) 310–311.
[16] S. Cheng, Y. Zhao, Y. Guo, Y. Li, Q. Wei, X.L. Wang, Y. Ren, P.K. Liaw, H. Choo, E.J. Lavernia, Adv. Mater. 21 (2009) 5001–5004.
[17] L. Lu, M.L. Sui, K. Lu, Science 287 (2000) 1463–1466.
[18] T.H. Fang, W.L. Li, N.R. Tao, K. Lu, Science 331 (2011) 1587–1590.
[19] D.S. Gianola, S. Van Petegem, M. Legros, S. Brandstetter, H. Van Swygenhoven, K.J. Hemker, Acta Mater. 54 (2006) 2253–2263.
[20] T.J. Rupert, D.S. Gianola, Y. Gan, K.J. Hemker, Science 326 (2009) 1686–1690.
[21] X.L. Wu, E. Ma, Appl. Phys. Lett. 88 (2006) 231911.
[22] X. Wu, Y. Zhu, Y. Wei, Q. Wei, Phys. Rev. Lett. 103 (2009) 205504.
[23] S. Ni, Y. Wang, X. Liao, S. Alhajeri, H. Li, Y. Zhao, E. Lavernia, S. Ringer, T. Langdon, Y. Zhu, Scr. Mater. 64 (2011) 327–330.
[24] M. Velasco, H. Van Swygenhoven, C. Brandl, Scr. Mater. 65 (2011) 151–154.
[25] J. Schäfer, K. Albe, Acta Mater. 60 (2012) 6076–6085.
[26] F. Sansoz, V. Dupont, Appl. Phys. Lett. 89 (2006) 111901.
[27] F. Mompiou, D. Caillard, M. Legros, Acta Mater. 57 (2009) 2198–2209.
[28] M. Legros, D.S. Gianola, K.J. Hemker, Acta Mater. 56 (2008) 3380–3393.
[29] M. Jin, A.M. Minor, E.A. Stach, J.W. Morris, Acta Mater. 52 (2004) 5381–5387.
[30] J. Li, A.K. Soh, Appl. Phys. Lett. 101 (2012) 241915.
[31] J.W. Cahn, J.E. Taylor, Acta Mater. 52 (2004) 4887–4898.
[32] J.W. Cahn, Y. Mishin, A. Suzuki, Acta Mater. 54 (2006) 4953–4975.
[33] T. Gorkaya, D.A. Molodov, G. Gottstein, Acta Mater. 57 (2009) 5396–5405.
[34] D. Caillard, F. Mompiou, M. Legros, Acta Mater. 57 (2009) 2390–2402.
[35] F. Mompiou, M. Legros, D. Caillard, Acta Mater. 58 (2010) 3676–3689.
[36] J. Li, A.K. Soh, Scr. Mater. 69 (2013) 283–286.
[37] J. Li, A.K. Soh, Acta Mater. 61 (2013) 5449–5457.
[38] J.T. De Hosson, W.A. Soer, A.M. Minor, Z. Shan, E.A. Stach, S.S. Asif, O.L. Warren, J. Mater. Sci. 41 (2006) 7704–7719.
[39] W.A. Soer, J.T.M. De Hosson, A.M. Minor, J.W. Morris, E.A. Stach, Acta Mater. 52 (2004) 5783–5790.
[40] F. Mompiou, D. Caillard, M. Legros, H. Mughrabi, Acta Mater. 60 (2012) 3402–3414.
[41] I.A. Ovid'ko, N.V. Skiba, Scr. Mater. 67 (2012) 13–16.
[42] M. Gutkin, I. Ovid'ko, Plastic Deformation in Nanocrystalline Materials, Springer, Berlin, 2004.
[43] A.E. Romanov, A.L. Kolesnikova, Prog. Mater. Sci. 54 (2009) 740–769.
[44] W.F. Gale, T.C. Totemeier, Smithells Metals Reference Book, 8th ed., Butterworth-Heinemann, Oxford, 2003.
[45] Y.T. Zhu, X.Z. Liao, S.G. Srinivasan, Y.H. Zhao, M.I. Baskes, F. Zhou, E.J. Lavernia, Appl. Phys. Lett. 85 (2004) 5049–5051.
[46] K. Youssef, M. Sakaliyska, H. Bahmanpour, R. Scattergood, C. Koch, Acta Mater. 59 (2011) 5758–5764.
[47] K. Zhang, I. Alexandrov, R. Valiev, K. Lu, J. Appl. Phys. 80 (1996) 5617–5624.